The Default Network of the Brain

7

Koene R. A. Van Dijk and Alexander Drzezga

Contents

Abstract

Continued advancement of sophisticated imaging procedures over the last decades has allowed the assessment of large-scale functional-anatomic brain networks. Among the identified networks, a frequently investigated system is the so-called default network. This network was originally identified as a set of brain regions consistently deactivated during tasks that require externally oriented attention. Later imaging studies showed that this network is active during inter-

K. R. A. Van Dijk (✉)
Digital Medicine and Translational Imaging, Early Clinical Development, Pfizer Inc, Cambridge, MA, USA
e-mail: koene.vandijk@pfizer.com

A. Drzezga
Department of Nuclear Medicine, Medical Faculty and University Hospital Cologne, University of Cologne, Cologne, Germany

German Center for Neurodegenerative Diseases (DZNE), Bonn/Köln, Germany

Institute of Neuroscience and Medicine, Molecular Organization of the Brain (INM-2), Forschungzentrum Jülich, Jülich, Germany
e-mail: alexander.drzezga@uk-koeln.de

R. A. J. O. Dierckx et al. (eds.), *PET and SPECT in Neurology*,
https://doi.org/10.1007/978-3-030-53168-3_7

nally focused cognitive processes such as moral decision-making and planning of future behavior, and also that it can reliably be identified during resting conditions. A growing number of studies indicate that various brain disorders are associated with dysfunction of brain networks, leading to the notion that measures of functional network integrity may serve as marker of neurologic and psychiatric disease states. For instance, disconnection of default network regions seems evident in very early stages of Alzheimer's disease, and a striking topographical overlap has been shown between default network regions and the spatial distribution of different diagnostic markers of Alzheimer's disease such as amyloid deposition, hypometabolism, and brain atrophy. In this chapter, we cover milestones that led to the discovery of the default network, methodological advancements that allow more precise measurements of neuronal networks, pitfalls of functional network measures, and a number of potential clinical applications.

7.1 Discovery of the Default Network

The set of brain regions we refer to as the *default network*, or *default mode network*, was first noted as a by-product of experiments aimed at mapping human brain function. In experiments that were common in the 1990s, positron emission tomography (PET) with suitable tracers (e.g., $H_2{}^{15}O$) or functional magnetic resonance imaging (fMRI) making use of the blood oxygenation level-dependent (BOLD) contrast was used to measure changes in regional cerebral blood flow. Before these neuroimaging techniques were available, basic research into brain function would consist of animal experiments with more or less successful translation to humans. Clinical research in those days was aimed at determining cognitive deficits in patients with known focal brain damage. The use of PET and fMRI for mapping cognitive functions turned out immensely successful because using these imaging techniques, scientists were able to determine fairly precisely the location of neuronal correlates of cognition in healthy study subjects. In a typical task-based experiment, or activation study, healthy young adults would perform a cognitive task in the scanner. Brain images acquired during, for instance, a language task would then be compared with brain images acquired during a reference condition that often consisted of simply resting in the scanner. Based on the theory of neurovascular coupling, brain regions with *higher* blood flow during the task would then be considered *activated* by the task. Thus, in the example of a language task, areas of the brain showing statistically higher signal during the language task would be attributed to language function.

Using neuroimaging techniques such as PET and fMRI, most researchers were initially focused on brain regions that showed higher levels of blood flow or oxygenation during specific tasks. However, Shulman et al. (1997) reported that during a number of different tasks (object discrimination, visual search, spatial attention, language, memory, and imagery), one particular set of brain regions would consistently show *lower* levels of blood flow during the tasks (see Fig. 7.1a). Blood flow

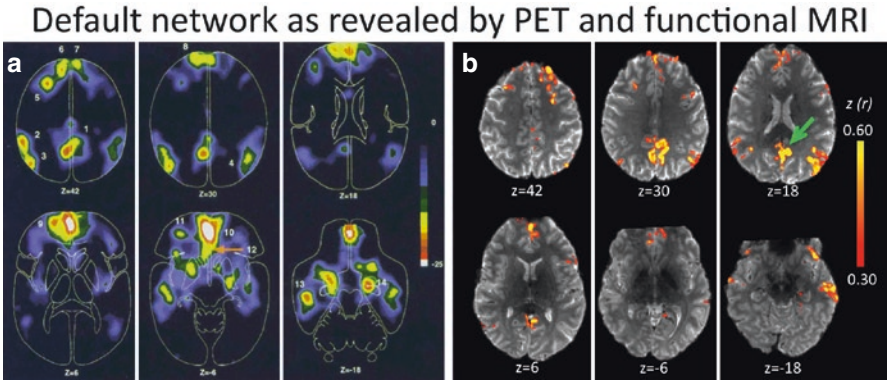

Fig. 7.1 (**a**) The default network of the human brain as it was originally identified in a meta-analysis of nine positron emission tomography (*PET*) studies (132 healthy young adults) from Shulman et al. (1997) (Reprinted with permission). The colored brain regions were more active in passive task states as compared to active tasks states. (**b**) The default network identified using functional connectivity MRI (fcMRI) while a single subject was resting in the scanner. The color scale indicates functional connectivity (Pearson correlation coefficient after Fishers *r*-to-*z* transformation) with the signal from a seed region placed in the posterior cingulate cortex as indicated by the *green arrow* (Adapted from Van Dijk et al. (2012b))

decreases during attention-demanding tasks were interpreted as decreases in brain activation, also referred to as deactivation. These consistent decreases during tasks suggested the existence of an organized functional-anatomic network that is more active during passive task conditions. Since humans are most of the time not engaged in attention-demanding goal-directed behavior, Raichle and colleagues referred to this network as representing a "default mode of brain function" (Raichle et al. 2001). After the publication by Raichle et al., the field started to refer to this set of brain regions as the "default network" or "default mode network." Greicius et al. (2003) showed that regions of the default network not only appear as deactivated regions during most attention-demanding cognitive tasks but in addition show high functional coherence while people are simply resting in the scanner (see Fig. 7.1b).

Brain regions associated with the default network are the posterior cingulate cortex, medial prefrontal cortex, inferior parietal lobule, lateral temporal cortex, and regions of the parahippocampal and entorhinal cortex (Buckner et al. 2008; Greicius et al. 2003; Raichle et al. 2001; Shulman et al. 1997; Ward et al. 2014). The relative ease of measuring this network during rest using standard neuroimaging techniques, in combination with initial findings of vulnerability of the default network to neurologic and psychiatric disease states, caused the default network to be a popular brain network to study which, in turn, led to an explosion of the number of papers on this topic published each year (see Fig. 7.2).

There is a growing interest in measuring structural connectivity of the default network and of other neuronal systems. While measures of brain structure, such as structural brain connectivity using diffusion magnetic resonance imaging, are beyond the scope of the present chapter, we would like to mention that several large

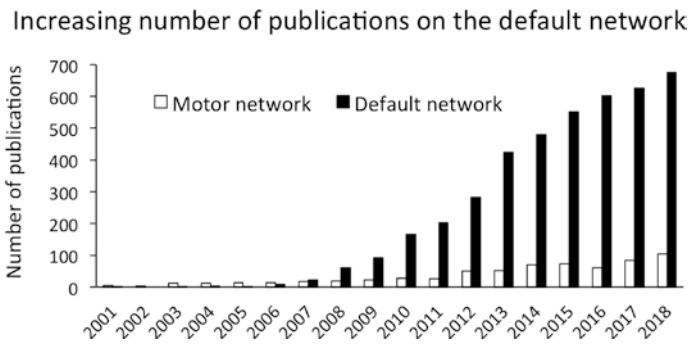

Fig. 7.2 There has been a steady increase in the number of papers published on the default network since the publication by Raichle et al. (2001) in which the term default mode was associated with the network described by Shulman et al. (1997). The graph shows the number of publications per year from 2001 until 2018 for the search terms ["motor network" OR "somatomotor network"](open bars) and ["default network" OR "default mode network" (closed bars)] (source https://www.ncbi.nlm.nih.gov/pubmed/, December 1, 2019)

multisite collaborative projects, such as the "Human Connectome Project" in the United States and the "Developing Human Connectome Project," "Human Brain Project," and the "UK Biobank" in Europe, are expected to shed more light on the complex relationship between brain structure and function during health and disease states.

7.2 Measuring Default Network Function

The main methods to assess default network function are (1) observing regions of deactivation during attention-demanding cognitive tasks, (2) probing the network with tasks that specifically rely on default network activation, (3) assessment of functional connectivity in terms of coherent BOLD fMRI signals either during task states or during the resting state, and finally (4) using FDG-PET to determine the molecular function and metabolic connectivity.

7.2.1 Deactivation During Attention-Demanding Cognitive Tasks

While the most commonly used clinical radiotracer for the assessment of brain function is ^{18}F-FDG (18-fluorodeoxyglucose for measuring glucose consumption), scientific activation studies performed in healthy young adults in the late 1980s and into the 1990s primarily used $H_2{}^{15}O$ (oxygen-15-water for measuring cerebral blood flow). Those studies were aimed at mapping cognitive functions such as language and decision-making under attention-demanding experimental conditions. The half-life of $H_2{}^{15}O$ is only 122 s (as opposed to 110 min for ^{18}F-FDG), which made it

suitable for repeated assessment of blood flow during different experimental conditions within one scanning session. Using $H_2{}^{15}O$-PET, many brain regions were identified that were implicated in a range of cognitive abilities. As mentioned in the previous section, an analysis by Shulman et al. (1997) of data of several PET experiments indicated that a common set of brain regions—which was only later termed the default network—showed consistent deactivation during various attention-demanding cognitive tasks. This means that those regions are more active in passive task conditions relative to many active task states. When it turned out that changes in blood oxygenation, as indirect measure of neuronal function, could be determined using BOLD fMRI without the use of radiotracers (Kwong et al. 1992; Ogawa et al. 1992), fMRI became the method of choice for studying brain function in healthy young adults. Parametric manipulation of task difficulty during BOLD fMRI experiments confirmed that the more a person is focused on an attention-demanding task, the more deactivation of the default network occurs (McKiernan et al. 2003).

7.2.2 Tasks That Rely on Default Network Activation

In addition to attention-demanding tasks that deactivate the default network, one can also ask people to perform tasks in the scanner that specifically *activate* the default network. Tasks relying on conceptual knowledge, moral decision-making, the ability to think what other people are thinking (i.e., theory of mind), remembering the past, and imagining the future are all associated with activation of default network regions and are therefore considered core functions of the network (e.g., Addis et al. 2007; Binder et al. 1999; Buckner et al. 2008; Mitchell et al. 2006; Shenhav and Greene 2012). Another suggested role of the default network is the exploratory monitoring of the external environment, a function that is suspended when a person is engaged in a task that requires focused attention (Gusnard et al. 2001; Shulman et al. 1997). In situations when people are left to think to themselves, the default network seems to integrate information from past experiences, replay events from memory, and construct mental simulations about possible future events (Buckner et al. 2008; Schacter et al. 2007).

7.2.3 Assessment of Functional Connectivity

Functional connectivity, defined as temporally correlated remote neurophysiological events (Friston 1994), can be estimated within individual subjects using functional neuroimaging measures such as EEG, MEG, and fMRI. The most commonly used method for assessing brain functional connectivity is fMRI and is often referred to as functional connectivity MRI (fcMRI). Using fcMRI, patterns of synchronous fluctuations in the blood oxygenation level-dependent (BOLD) signal are measured (Biswal et al. 1995). These analyses involve data processing, including steps to remove unwanted signals such as physiological noise caused by heart rate,

breathing, and head motion. If, after data preprocessing, two or more brain regions show a similar pattern in fluctuations over time, we designate these regions as being functionally connected. While functional connectivity does not equate to structural connectivity, fcMRI can be used as noninvasive probe of integrity of neuronal systems (for review, see Van Dijk et al. 2010).

Biswal and colleagues in 1995 used BOLD fMRI to show that a region in the left somatomotor cortex exhibits signal fluctuations that are highly correlated with signal fluctuations in the whole somatomotor system including contralateral somatomotor cortex (Biswal et al. 1995). It is important to realize that the somatomotor system exhibits these coherent signal fluctuations when a person is simply resting in the scanner, that is, when a person is not engaged in active behavior that relies on the somatomotor system. This technique of mapping functional systems by analyzing coherent fluctuations in remote brain areas increased in popularity when Greicius et al. (2003) decided to place a region of interest—also called a "seed region"—in a core node of the default network. When they extracted the signal from that seed region and computed the correlation strength between the seed and every other voxel in the brain, the results robustly revealed the default network (Greicius et al. 2003). During those years, data-driven techniques that do not rely on choosing a specific seed region also revealed coherent activity patterns in large-scale brain systems such as the somatomotor and default network (Beckmann et al. 2005; De Luca et al. 2006). While it is relatively easy to measure these networks while people are resting in the scanner, it is important to note that most networks, including the default network, also show functional connectivity during many tasks (Fransson 2006; Smith et al. 2009; Van Dijk et al. 2010). This means that functional connectivity methods can be applied to data acquired during rest but also during active task conditions (for applications and discussion, see Fair et al. (2007). When one is interested in how functional connectivity changes during different conditions of a task, other methods, such as psychophysiological interaction analysis, are suitable (Friston et al. 1997; McLaren et al. 2012).

Over the last years, different authors have focused on different networks as measured during rest. Besides the default network, often-mentioned systems are those involved in keeping attention focused on a task (dorsal attention network or salience network; see, e.g., Fox et al. 2005 and Seeley et al. 2007, respectively) or networks performing executive control functions such as allocating attention to one stimulus and then actively switching attention to another stimulus when cued to do so (Seeley et al. 2007; Vincent et al. 2008). Efforts of determining an exact number of meaningful neuronal networks will offer different results based on the methods employed and the behavior of the subject during the scan. Moreover, while these fcMRI metrics show fairly stable measurements from one session to the next (e.g., Shehzad et al. 2009; Van Dijk et al. 2010), the correlational measures do not capture moment-to-moment changes in coherence (Chang and Glover 2010; Hutchison et al. 2013; Lurie et al. 2020).

Potential pitfalls when using fcMRI to determine functional network integrity are contamination of the BOLD signal by the before-mentioned sources of

physiological noise such as heart rate, respiration (Birn et al. 2006; Chang and Glover 2009), and head motion (Power et al. 2012; Satterthwaite et al. 2012; Van Dijk et al. 2012a). It is crucial that investigators that apply fcMRI are aware of these confounding factors since they often bias results in studies where patients are compared to healthy controls in the direction of hypothesized effects. For instance, one might find lower coherence in the default network in the patient group which may not be due to a specific brain disorder but rather to more head movement in the patient group during the scan. Discussion of additional caveats when working with measures of functional network integrity and interpretation of functional network changes when structural brain changes are also present are beyond the scope of this chapter but are topics of active research.

With the increasing availability of high-quality neuroimaging datasets and advances in computational approaches to complex biological systems, a field has emerged in which the brain is treated as graph with brain regions as nodes and functional or structural connections as edges or links between the nodes (Bullmore and Sporns 2009; Drzezga et al. 2011; Rubinov and Sporns 2010; Sepulcre et al. 2010; Stam and Reijneveld 2007; van den Heuvel et al. 2008). Graph theory applied to structural and functional brain images has shown that the human brain is shaped by an economic trade-off between minimizing costs and maximizing efficiency of information processing whereby the brain exhibits properties of a *complex network* that sits in between a regular low-cost/low-efficiency lattice network and a high-cost/high-efficiency random network (see Fig. 7.3).

While complex brain network analysis techniques often take the whole brain into account and are not necessarily aimed at identifying (just) the default network, it turns out that the brain's main cortical hubs largely—but not fully—overlap with

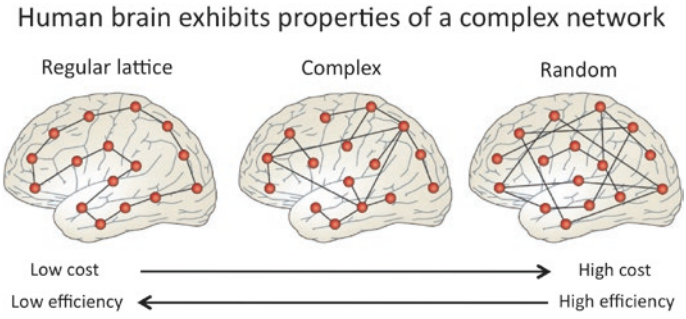

Fig. 7.3 The human brain exhibits properties of a complex network that sits in between an orderly regular lattice structure and an unorderly random network. The healthy human brain shows a balance between minimizing costs and maximizing processing efficiency. While the default network is known to include many key relay stations that are important for this cost/efficiency trade-off, graph theoretical measures of the human brain go beyond the default network and are starting to show promise to identify changes in brain network structure in neurologic and psychiatric disease states (Adapted with permission from Macmillan Publishers Ltd.: Nature Reviews Neuroscience, Bullmore and Sporns, copyright 2012)

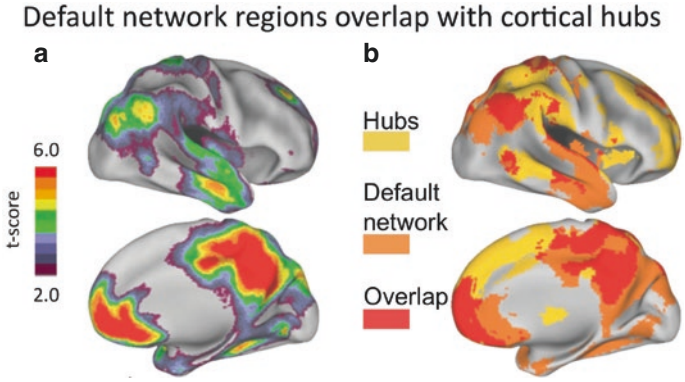

Fig. 7.4 (**a**) Map of the default network as voxels exhibiting greater activity during blocks of passive fixation than during externally directed tasks. Six independent fMRI blocked-design studies were included, each comprising 30 participants matched on age and gender for a total of 180 healthy young adults. The scale is average *t*-score. The map of the default network is consistent with prior meta-analyses (e.g., Shulman et al. (1997) as shown in Fig. 7.1a). (**b**) Overlap of the default network with a map of degree connectivity representing cortical hubs (Adapted with permission from Buckner et al. (2009))

default network regions (see Fig. 7.4). One potential role of these hub regions is that they act as relay stations for information processing serving as connector regions between different (sub)networks. Other complex brain network analyses suggest that default network regions display extensive local connectivity between and within certain bordering brain areas (see Buckner et al. 2009; Sepulcre et al. 2010; Tomasi and Volkow 2010 for discussion). Complex brain network analysis relies first on time-series analyses within an individual subject, but the next step requires analyses of patters across large groups of subjects. This may have utility in detecting abnormal connectomics due to neurologic and psychiatric disease states (Bullmore and Sporns 2012; Rubinov and Sporns 2010; Dichter et al. 2015; Derks et al. 2017), but the practical utility of network measures for diagnostic and/or treatment decisions within an individual patient remains to be determined.

7.2.4 Molecular Function and Metabolic Connectivity

The abovementioned fcMRI methods rely on functional connectivity between brain regions to be estimated within individual subjects. ^{18}F-FDG-PET traditionally does not provide information regarding change in neuronal function over time but rather offers a snapshot reflecting synaptic glutamatergic activity which then serves as summary measure of neuronal function over the duration of the scan. This means that within one subject, connectivity between two given regions (region A and B) cannot be computed using traditional FDG-PET as in both regions only a single value will be obtained. However, a correlation between the values in region A can be computed with the values in region B across subjects. This approach using PET

was used before the availability of fMRI BOLD methods (e.g., Horwitz et al. 1984; McIntosh 1999), and the same concept has successfully been applied to structural MRI data of older adults with and without dementia (e.g., He et al. 2008; Seeley et al. 2009). Across-subject analysis of FDG-PET data has been termed "metabolic connectivity" in a study by Morbelli et al. (2012), in which they demonstrated reduced resting metabolic connectivity in prodromal Alzheimer's disease both in hypometabolic and non-hypometabolic areas and they suggested that metabolic disconnection (reflecting early diaschisis) may antedate remote hypometabolism (early sign of synaptic degeneration) (Morbelli et al. 2012).

Thanks to increasing temporal resolution of modern PET imaging systems, metabolic connectivity can now also be studied within a single subject or patient using functional PET (fPET; Villien et al. 2014). This method employs a constant infusion of radiotracer and enables assessment of changes in brain metabolism over the course of a task paradigm or during resting-state conditions.

7.2.5 Clinical Relevance of Measuring Default Network Integrity

There are several lines of evidence indicating that default network integrity may serve as marker of brain function with relevance for several neurologic and psychiatric disease states (for review, see Fox and Greicius 2010; Teipel et al. 2016). One example where loss of deactivation during task conditions and disconnection measured during resting-state conditions across the spectrum of prodromal and clinical disease phases is Alzheimer's disease. Loss of task-related deactivation in Alzheimer's disease was shown for the default network using fMRI (Lustig et al. 2003) and for other association regions using $H_2{}^{15}O$ PET (Drzezga et al. 2005). With the development of PET tracers such as ^{11}C-Pittsburgh compound B (11C-PiB; Klunk et al. 2004; Mathis et al. 2004), in vivo measurement of fibrillar amyloid beta, one of the major neuropathological hallmarks of Alzheimer's disease, became possible. It turned out that older adults who presented with elevated ^{11}C-PiB uptake, but who were otherwise still cognitively normal, showed loss of deactivation of the default network during fMRI task performance (Sperling et al. 2009).

In situations where patients may have difficulty performing a cognitive task in the scanner, or in multisite collaborative studies where it is difficult to implement a behavioral task protocol and monitor task compliance, a resting-state fMRI scan has been shown to be useful. Disconnection of regions of the default network during rest has been reported in Alzheimer's disease (Greicius et al. 2004) and also in patients who are at high risk of developing the disease (Filippini et al. 2009; Sorg et al. 2007). In addition, even older adults who show no clinical signs of Alzheimer's disease but who have elevated amyloid values as measured using ^{11}C-PiB-PET showed decreases in fcMRI measures of the default network (Hedden et al. 2009; Mormino et al. 2011; Sheline et al. 2010). Finally, regional overlap of default network disconnection, amyloid burden, and neuronal dysfunction was shown using resting-state fcMRI, ^{11}C-PiB-PET, and ^{18}F-FDG-PET, respectively (Drzezga et al. 2011), lending support to the hypothesis that

Alzheimer's disease-associated amyloid deposition tends to concentrate in default network areas (Buckner et al. 2005) or more generally in functional hubs of the brain that overlap with typical default network areas and other critical nodes of large-scale functional networks (Buckner et al. 2009). These findings indicate that assessment of the default mode network and other major neuronal networks may serve as marker of functional brain integrity, prior to occurrence of symptoms of memory loss due to Alzheimer's disease-related pathology and also prior to anatomical changes that will only later become visible with structural brain imaging techniques (Sperling et al. 2011).

Availability of in vivo assessment of tau aggregates using tracers such as ^{18}F-AV-1451 (T807; Chien et al. 2013; Xia et al. 2013) as well as adaptation of PET tau imaging in large longitudinal cohort studies such as the Alzheimer's Disease Neuroimaging Initiative (ADNI) has offered a view that multiple networks may be differentially affected by pathologies that may show its effects at different (pre) clinical disease stages (see, e.g., Jones et al. 2017; Hoenig et al. 2018; Sepulcre et al. 2018).

Applying PET tracers for imaging amyloid and tau deposition in the brain, recent studies were able to identify characteristic networks of amyloid deposition in the brain as well as specific "tau networks" of tau distribution in patients with Alzheimer's disease (Pereira et al. 2018; Kim et al. 2019; Hoenig et al. 2018). Substantial overlap between amyloid deposition, tau aggregation, and functional-anatomic networks was demonstrated, particularly for the default network. These findings indicate that Alzheimer pathology shows a preference for development within the default network, potentially due to high susceptibility of this network and potential spreading of the molecular pathologies along its connectivity pathways. These findings have further fueled the so-called network degeneration hypothesis, postulating that neurodegenerative disorders are possibly characterized by the way molecular pathologies are spreading along functional networks of the brain (see, for review, Drzezga 2018).

It is unlikely that default network dysfunction is exclusively indicative of (preclinical) Alzheimer's disease because this network has been implicated in a range of different conditions (for an early review, see Fox and Greicius 2010). In addition, most studies referenced in this chapter showed functional network characteristics based on group averages of normal control subjects or group differences between patients and controls, but it has become clear that these large-scale functional networks, when measured at high spatial resolution in individual subjects, show consistent fractionation within individuals (Braga et al. 2019) of which clinical utility remains to be determined. In the coming years, we will likely learn more about sensitivity and specificity of measures of neuronal network dysfunction and its clinical utility in a range of different conditions.

Besides investigating which neurologic and psychiatric disease affects which brain system, there are a number of other clinical applications for measuring the connectional architecture of the brain. One such example is presurgical mapping of functional brain areas in patients that might otherwise be scanned while performing a task but who have difficulty with task comprehension and/or task compliance (Liu

et al. 2009; Lee et al. 2016) with recent publications confirming utility but also calling for further investigations into subject-level variability before widespread clinical implementation (Sair et al. 2017). Another potential clinical application is determining brain function in individual patients with disorders of consciousness where a minimal conscious state might be differentiated from vegetative state using default network measures (Fernandez-Espejo et al. 2012). And finally, resting-state functional network measures have been used for image-guided manipulation using transcranial magnetic stimulation (TMS) of brain networks in psychiatric diseases (Fox et al. 2012). With continued efforts of improved data acquisition and analysis techniques, including higher spatial and temporal resolution MRI (Smith et al. 2011; Triantafyllou et al. 2005; Setsompop et al. 2012; Van Dijk et al. 2012b), and simultaneous PET/MR data acquisition (Heiss 2009; Marsden et al. 2002), additional translational research for clinical applications is likely to follow.

References

Addis DR, Wong AT, Schacter DL (2007) Remembering the past and imagining the future: common and distinct neural substrates during event construction and elaboration. Neuropsychologia 45:1363–1377

Beckmann CF, DeLuca M, Devlin JT, Smith SM (2005) Investigations into resting-state connectivity using independent component analysis. Philos Trans R Soc Lond Ser B Biol Sci 360:1001–1013

Binder JR, Frost JA, Hammeke TA, Bellgowan PS, Rao SM, Cox RW (1999) Conceptual processing during the conscious resting state. A functional MRI study. J Cogn Neurosci 11:80–95

Birn RM, Diamond JB, Smith MA, Bandettini PA (2006) Separating respiratory-variation-related fluctuations from neuronal-activity-related fluctuations in fMRI. NeuroImage 31:1536–1548

Biswal B, Yetkin FZ, Haughton VM, Hyde JS (1995) Functional connectivity in the motor cortex of resting human brain using echo-planar MRI. Magn Reson Med 34:537–541

Braga RM, Van Dijk KRA, Polimeni JR, Eldaief MC, Buckner RL (2019) Parallel distributed networks resolved at high resolution reveal close juxtaposition of distinct regions. J Neurophysiol 121(4):1513–1534

Buckner RL, Snyder AZ, Shannon BJ, LaRossa G, Sachs R, Fotenos AF, Sheline YI, Klunk WE, Mathis CA, Morris JC et al (2005) Molecular, structural, and functional characterization of Alzheimer's disease: evidence for a relationship between default activity, amyloid, and memory. J Neurosci 25:7709–7717

Buckner RL, Andrews-Hanna JR, Schacter DL (2008) The brain's default network: anatomy, function, and relevance to disease. Ann N Y Acad Sci 1124:1–38

Buckner RL, Sepulcre J, Talukdar T, Krienen FM, Liu H, Hedden T, Andrews-Hanna JR, Sperling RA, Johnson KA (2009) Cortical hubs revealed by intrinsic functional connectivity: mapping, assessment of stability, and relation to Alzheimer's disease. J Neurosci 29:1860–1873

Bullmore E, Sporns O (2009) Complex brain networks: graph theoretical analysis of structural and functional systems. Nat Rev Neurosci 10:186–198

Bullmore E, Sporns O (2012) The economy of brain network organization. Nat Rev Neurosci 13:336–349

Chang C, Glover GH (2009) Relationship between respiration, end-tidal CO(2), and BOLD signals in resting-state fMRI. NeuroImage 47(4):1381–1393

Chang C, Glover GH (2010) Time-frequency dynamics of resting-state brain connectivity measured with fMRI. NeuroImage 50:81–98

Chien DT, Bahri S, Szardenings AK, Walsh JC, Mu F, Su MY, Shankle WR, Elizarov A, Kolb HC (2013) Early clinical PET imaging results with the novel PHF-tau radioligand [F-18]-T807. J Alzheimers Dis 34:457–468

De Luca M, Beckmann CF, De Stefano N, Matthews PM, Smith SM (2006) fMRI resting state networks define distinct modes of long-distance interactions in the human brain. NeuroImage 29:1359–1367

Derks J, Dirkson AR, de Witt Hamer PC, van Geest Q, Hulst HE, Barkhof F, Pouwels PJ, Geurts JJ, Reijneveld JC, Douw L (2017) Connectomic profile and clinical phenotype in newly diagnosed glioma patients. Neuroimage Clin 14:87–96

Dichter GS, Gibbs D, Smoski MJ (2015) A systematic review of relations between resting-state functional-MRI and treatment response in major depressive disorder. J Affect Disord 172:8–17

Drzezga A (2018) The network degeneration hypothesis: spread of neurodegenerative patterns along neuronal brain networks. J Nucl Med 59:1645–1648

Drzezga A, Grimmer T, Peller M, Wermke M, Siebner H, Rauschecker JP, Schwaiger M, Kurz A (2005) Impaired cross-modal inhibition in Alzheimer disease. PLoS Med 2:e288

Drzezga A, Becker JA, Van Dijk KRA, Sreenivasan A, Talukdar T, Sullivan C, Schultz AP, Sepulcre J, Putcha D, Greve D et al (2011) Neuronal dysfunction and disconnection of cortical hubs in non-demented subjects with elevated amyloid burden. Brain 134:1635–1646

Fair DA, Schlaggar BL, Cohen AL, Miezin FM, Dosenbach NU, Wenger KK, Fox MD, Snyder AZ, Raichle ME, Petersen SE (2007) A method for using blocked and event-related fMRI data to study "resting state" functional connectivity. NeuroImage 35:396–405

Fernandez-Espejo D, Soddu A, Cruse D, Palacios EM, Junque C, Vanhaudenhuyse A, Rivas E, Newcombe V, Menon DK, Pickard JD et al (2012) A role for the default mode network in the bases of disorders of consciousness. Ann Neurol 72:335–343

Filippini N, MacIntosh BJ, Hough MG, Goodwin GM, Frisoni GB, Smith SM, Matthews PM, Beckmann CF, Mackay CE (2009) Distinct patterns of brain activity in young carriers of the APOE-epsilon4 allele. Proc Natl Acad Sci U S A 106:7209–7214

Fox MD, Buckner RL, White MP, Greicius MD, Pascual-Leone A (2012) Efficacy of transcranial magnetic stimulation targets for depression is related to intrinsic functional connectivity with the subgenual cingulate. Biol Psychiatry 72(7):595–603

Fox MD, Greicius M (2010) Clinical applications of resting state functional connectivity. Front Syst Neurosci 4:19. https://doi.org/10.3389/fnsys.2010.00019

Fox MD, Snyder AZ, Vincent JL, Corbetta M, Van Essen DC, Raichle ME (2005) The human brain is intrinsically organized into dynamic, anticorrelated functional networks. Proc Natl Acad Sci U S A 102:9673–9678

Fransson P (2006) How default is the default mode of brain function? Further evidence from intrinsic BOLD signal fluctuations. Neuropsychologia 44:2836–2845

Friston KJ (1994) Functional and effective connectivity in neuroimaging: a synthesis. Hum Brain Mapp 2:56–87

Friston KJ, Buechel C, Fink GR, Morris J, Rolls E, Dolan RJ (1997) Psychophysiological and modulatory interactions in neuroimaging. NeuroImage 6:218–229

Greicius MD, Krasnow B, Reiss AL, Menon V (2003) Functional connectivity in the resting brain: a network analysis of the default mode hypothesis. Proc Natl Acad Sci U S A 100:253–258

Greicius MD, Srivastava G, Reiss AL, Menon V (2004) Default-mode network activity distinguishes Alzheimer's disease from healthy aging: evidence from functional MRI. Proc Natl Acad Sci U S A 101:4637–4642

Gusnard DA, Raichle ME, Raichle ME (2001) Searching for a baseline: functional imaging and the resting human brain. Nat Rev Neurosci 2:685–694

He Y, Chen Z, Evans A (2008) Structural insights into aberrant topological patterns of large-scale cortical networks in Alzheimer's disease. J Neurosci 28:4756–4766

Hedden T, Van Dijk KRA, Becker JA, Mehta A, Sperling RA, Johnson KA, Buckner RL (2009) Disruption of functional connectivity in clinically normal older adults harboring amyloid burden. J Neurosci 29:12686–12694

Heiss WD (2009) The potential of PET/MR for brain imaging. Eur J Nucl Med Mol Imaging 36(Suppl 1):S105–S112

Hoenig MC, Bischof GN, Seemiller J, Hammes J, Kukolja J, Onur ÖA, Jessen F, Fliessbach K, Neumaier B, Fink GR, van Eimeren T, Drzezga A (2018) Networks of tau distribution in Alzheimer's disease. Brain 141(2):568–581

Horwitz B, Duara R, Rapoport SI (1984) Intercorrelations of glucose metabolic rates between brain regions: application to healthy males in a state of reduced sensory input. J Cereb Blood Flow Metab 4:484–499

Hutchison RM, Womelsdorf T, Allen EA, Bandettini PA, Calhoun VD, Corbetta M, Della Penna S, Duyn JH, Glover GH, Gonzalez-Castillo J, Handwerker DA, Keilholz S, Kiviniemi V, Leopold DA, de Pasquale F, Sporns O, Walter M, Chang C (2013) Dynamic functional connectivity: promise, issues, and interpretations. NeuroImage 80:360–378

Jones DT, Graff-Radford J, Lowe VJ, Wiste HJ, Gunter JL, Senjem ML, Botha H, Kantarci K, Boeve BF, Knopman DS, Petersen RC, Jack CR Jr (2017) Tau, amyloid, and cascading network failure across the Alzheimer's disease spectrum. Cortex 97:143–159

Kim J, Ghadery C, Cho SS, Mihaescu A, Christopher L, Valli M, Houle S, Strafella AP (2019) Network patterns of Beta-amyloid deposition in Parkinson's disease. Mol Neurobiol 56:7731–7740

Klunk WE, Engler H, Nordberg A, Wang Y, Blomqvist G, Holt DP, Bergström M, Savitcheva I, Huang GF, Estrada S, Ausén B, Debnath ML, Barletta J, Price JC, Sandell J, Wall A, Koivisto P, Antoni G, Mathis CA, Långström B (2004) Imaging brain amyloid in Alzheimer's disease with Pittsburgh compound-B. Ann Neurol 55:306–319

Kwong KK, Belliveau JW, Chesler DA, Goldberg IE, Weisskoff RM, Poncelet BP, Kennedy DN, Hoppel BE, Cohen MS, Turner R et al (1992) Dynamic magnetic resonance imaging of human brain activity during primary sensory stimulation. Proc Natl Acad Sci U S A 89:5675–5679

Lee MH, Miller-Thomas MM, Benzinger TL, Marcus DS, Hacker CD, Leuthardt EC, Shimony JS (2016) Clinical resting-state fMRI in the preoperative setting: are we ready for prime time? Top Magn Reson Imaging 25(1):11–18

Liu H, Buckner RL, Talukdar T, Tanaka N, Madsen JR, Stufflebeam SM (2009) Task-free presurgical mapping using functional magnetic resonance imaging intrinsic activity. J Neurosurg 111(4):746–754

Lurie DJ, Kessler D, Bassett DS, Betzel RF, Breakspear M, Keilholz S et al (2020) Questions and controversies in the study of time-varying functional connectivity in resting fMRI. Netw Neurosci 4(1):30–69. https://doi.org/10.1162/netn_a_00116

Lustig C, Snyder AZ, Bhakta M, O'Brien KC, McAvoy M, Raichle ME, Morris JC, Buckner RL (2003) Functional deactivations: change with age and dementia of the Alzheimer type. Proc Natl Acad Sci U S A 100:14504–14509

Marsden PK, Strul D, Keevil SF, Williams SC, Cash D (2002) Simultaneous PET and NMR. Br J Radiol 75:S53–S59

Mathis CA, Wang Y, Klunk WE (2004) Imaging beta-amyloid plaques and neurofibrillary tangles in the aging human brain. Curr Pharm Des 10:1469–1492

McIntosh AR (1999) Mapping cognition to the brain through neural interactions. Memory 7:523–548

McKiernan KA, Kaufman JN, Kucera-Thompson J, Binder JR (2003) A parametric manipulation of factors affecting task-induced deactivation in functional neuroimaging. J Cogn Neurosci 15:394–408

McLaren DG, Ries ML, Xu G, Johnson SC (2012) A generalized form of context-dependent psychophysiological interactions (gPPI): a comparison to standard approaches. NeuroImage 61:1277–1286

Mitchell JP, Macrae CN, Banaji MR (2006) Dissociable medial prefrontal contributions to judgments of similar and dissimilar others. Neuron 50:655–663

Morbelli S, Drzezga A, Perneczky R, Frisoni GB, Caroli A, van Berckel BN, Ossenkoppele R, Guedj E, Didic M, Brugnolo A et al (2012) Resting metabolic connectivity in prodromal Alzheimer's disease. A European Alzheimer Disease Consortium (EADC) project. Neurobiol Aging 33:2533–2550

Mormino EC, Smiljic A, Hayenga AO, Onami SH, Greicius MD, Rabinovici GD, Janabi M, Baker SL, Yen IV, Madison CM et al (2011) Relationships between beta-amyloid and functional connectivity in different components of the default mode network in aging. Cereb Cortex 21(10):2399–2407

Ogawa S, Tank DW, Menon RS, Ellermann JM, Kim SG, Merkle H, Ugurbil K (1992) Intrinsic signal changes accompanying sensory stimulation: functional brain mapping with magnetic resonance imaging. Proc Natl Acad Sci U S A 89:5951–5955

Pereira JB, Strandberg TO, Palmqvist S, Volpe G, van Westen D, Westman E, Hansson O, Alzheimer's Disease Neuroimaging Initiative (2018) Amyloid network topology characterizes the progression of Alzheimer's disease during the predementia stages. Cereb Cortex 28:340–349

Power JD, Barnes KA, Snyder AZ, Schlaggar BL, Petersen SE (2012) Spurious but systematic correlations in functional connectivity MRI networks arise from subject motion. NeuroImage 59:2142–2154

Raichle ME, MacLeod AM, Snyder AZ, Powers WJ, Gusnard DA, Shulman GL (2001) A default mode of brain function. Proc Natl Acad Sci U S A 98:676–682

Rubinov M, Sporns O (2010) Complex network measures of brain connectivity: uses and interpretations. NeuroImage 52:1059–1069

Satterthwaite TD, Wolf DH, Loughead J, Ruparel K, Elliott MA, Hakonarson H, Gur RC, Gur RE (2012) Impact of in-scanner head motion on multiple measures of functional connectivity: relevance for studies of neurodevelopment in youth. NeuroImage 60:623–632

Schacter DL, Addis DR, Buckner RL (2007) Remembering the past to imagine the future: the prospective brain. Nat Rev Neurosci 8:657–661

Sair HI, Agarwal S, Pillai JJ (2017) Application of resting state functional MR imaging to presurgical mapping: language mapping. Neuroimaging Clin N Am 27(4):635–644

Seeley WW, Menon V, Schatzberg AF, Keller J, Glover GH, Kenna H, Reiss AL, Greicius MD (2007) Dissociable intrinsic connectivity networks for salience processing and executive control. J Neurosci 27:2349–2356

Seeley WW, Crawford RK, Zhou J, Miller BL, Greicius MD (2009) Neurodegenerative diseases target large-scale human brain networks. Neuron 62:42–52

Sepulcre J, Grothe MJ, d'Oleire Uquillas F, Ortiz-Terán L, Diez I, Yang HS, Jacobs HIL, Hanseeuw BJ, Li Q, El-Fakhri G, Sperling RA, Johnson KA (2018) Neurogenetic contributions to amyloid beta and tau spreading in the human cortex. Nat Med 24(12):1910–1918

Sepulcre J, Liu H, Talukdar T, Martincorena I, Yeo BT, Buckner RL (2010) The organization of local and distant functional connectivity in the human brain. PLoS Comput Biol 6:e1000808

Setsompop K, Gagoski BA, Polimeni JR, Witzel T, Wedeen VJ, Wald LL (2012) Blipped-controlled aliasing in parallel imaging for simultaneous multislice echo planar imaging with reduced g-factor penalty. Magn Reson Med 67(5):1210–1224

Shehzad Z, Kelly AM, Reiss PT, Gee DG, Gotimer K, Uddin LQ, Lee SH, Margulies DS, Roy AK, Biswal BB et al (2009) The resting brain: unconstrained yet reliable. Cereb Cortex 19:2209–2229

Sheline YI, Raichle ME, Snyder AZ, Morris JC, Head D, Wang S, Mintun MA (2010) Amyloid plaques disrupt resting state default mode network connectivity in cognitively normal elderly. Biol Psychiatry 67:584–587

Shenhav A, Greene JD (2012) Moral judgments recruit domain-general valuation mechanisms to integrate representations of probability and magnitude. Neuron 67:667–677

Shulman GL, Fiez JA, Corbetta M, Buckner RL, Miezin FM, Raichle ME, Petersen SE (1997) Common blood flow changes across visual tasks: II.: decreases in cerebral cortex. J Cogn Neurosci 9:648–663

Smith SM, Fox PT, Miller KL, Glahn DC, Fox PM, Mackay CE, Filippini N, Watkins KE, Toro R, Laird AR et al (2009) Correspondence of the brain's functional architecture during activation and rest. Proc Natl Acad Sci U S A 106:13040–13045

Smith SM, Miller KL, Moeller S, Xu J, Auerbach EJ, Woolrich MW, Beckmann CF, Jenkinson M, Andersson J, Glasser MF et al (2011) Temporally-independent functional modes of spontaneous brain activity. Proc Natl Acad Sci U S A 109:3131–3136

Sorg C, Riedl V, Muhlau M, Calhoun VD, Eichele T, Laer L, Drzezga A, Forstl H, Kurz A, Zimmer C et al (2007) Selective changes of resting-state networks in individuals at risk for Alzheimer's disease. Proc Natl Acad Sci U S A 104:18760–18765

Sperling RA, Laviolette PS, O'Keefe K, O'Brien J, Rentz DM, Pihlajamaki M, Marshall G, Hyman BT, Selkoe DJ, Hedden T et al (2009) Amyloid deposition is associated with impaired default network function in older persons without dementia. Neuron 63:178–188

Sperling RA, Aisen PS, Beckett LA, Bennett DA, Craft S, Fagan AM, Iwatsubo T, Jack CR Jr, Kaye J, Montine TJ et al (2011) Toward defining the preclinical stages of Alzheimer's disease: recommendations from the National Institute on Aging-Alzheimer's association workgroups on diagnostic guidelines for Alzheimer's disease. Alzheimers Dement 7:280–292

Stam CJ, Reijneveld JC (2007) Graph theoretical analysis of complex networks in the brain. Nonlinear Biomed Phys 1:3

Teipel S, Grothe MJ, Zhou J, Sepulcre J, Dyrba M, Sorg C, Babiloni C (2016) Measuring cortical connectivity in Alzheimer's disease as a brain neural network pathology: toward clinical applications. J Int Neuropsychol Soc 22(2):138–163

Tomasi D, Volkow ND (2010) Functional connectivity density mapping. Proc Natl Acad Sci U S A 107:9885–9890

Triantafyllou C, Hoge RD, Krueger G, Wiggins CJ, Potthast A, Wiggins GC, Wald LL (2005) Comparison of physiological noise at 1.5 T, 3 T and 7 T and optimization of fMRI acquisition parameters. NeuroImage 26:243–250

van den Heuvel MP, Stam CJ, Boersma M, Hulshoff Pol HE (2008) Small-world and scale-free organization of voxel-based resting-state functional connectivity in the human brain. NeuroImage 43:528–539

Van Dijk KRA, Hedden T, Venkataraman A, Evans KC, Lazar SW, Buckner RL (2010) Intrinsic functional connectivity as a tool for human connectomics: theory, properties, and optimization. J Neurophysiol 103:297–321

Van Dijk KRA, Sabuncu MR, Buckner RL (2012a) The influence of head motion on intrinsic functional connectivity MRI. NeuroImage 59:431–438

Van Dijk KRA, Triantafyllou C, Keil B, Hedden T, Wald LL , Buckner RL (2012b) Detailed anatomical localization of intrinsic connectivity networks using high spatial resolution fMRI at 7 tesla. In: Neuroscience meeting planner. Program no. 79.13. 2012, New Orleans

Villien M, Wey HY, Mandeville JB, Catana C, Polimeni JR, Sander CY, Zürcher NR, Chonde DB, Fowler JS, Rosen BR, Hooker JM (2014) Dynamic functional imaging of brain glucose utilization using fPET-FDG. NeuroImage 100:192–199

Vincent JL, Kahn I, Snyder AZ, Raichle ME, Buckner RL (2008) Evidence for a frontoparietal control system revealed by intrinsic functional connectivity. J Neurophysiol 100:3328–3342

Ward A, Schultz AP, Huijbers W, Van Dijk KRA, Hedden T, Sperling RA (2014) The parahippocampal gyrus links the default mode cortical network with the medial temporal lobe memory system. Hum Brain Mapp 35(3):1061–1073

Xia CF, Arteaga J, Chen G, Gangadharmath U, Gomez LF, Kasi D, Lam C, Liang Q, Liu C, Mocharla VP, Mu F, Sinha A, Su H, Szardenings AK, Walsh JC, Wang E, Yu C, Zhang W, Zhao T, Kolb HC (2013) [(^{18})F]T807, a novel tau positron emission tomography imaging agent for Alzheimer's disease. Alzheimers Dement 9(6):666–676